creative commons
COMMONS DEED

저작자표시 2.0 대한민국

이용자는 아래의 조건을 따르는 경우에 한하여 자유롭게

- 이 저작물을 복제, 배포, 전송, 전시, 공연 및 방송할 수 있습니다.
- 이차적 저작물을 작성할 수 있습니다.
- 이 저작물을 영리 목적으로 이용할 수 있습니다.

다음과 같은 조건을 따라야 합니다:

저작자표시. 귀하는 원저작자를 표시하여야 합니다.

- 귀하는, 이 저작물의 재이용이나 배포의 경우, 이 저작물에 적용된 이용허락조건을 명확하게 나타내어야 합니다.
- 저작권자로부터 별도의 허가를 받으면 이러한 조건들은 적용되지 않습니다.

저작권법에 따른 이용자의 권리는 위의 내용에 의하여 영향을 받지 않습니다.

이것은 이용허락규약(Legal Code)을 이해하기 쉽게 요약한 것입니다.

Disclaimer

dCollection

[UCI]I804:24011-200000266854
조선대학교 CHOSUN UNIVERSITY

2018년 8월
석사학위논문
New metformin derivative HL156A prevents oral cancer progression by inhibiting the IGF/AKT/mTOR pathways
LAM THUY GIANG

2018년 8월

석사 학위 논문

New metformin derivative HL156A prevents oral cancer progression by inhibiting the IGF/AKT/mTOR pathways

조선대학교 대학원

치의생명공학과

LAM THUY GIANG

조선대학교
CHOSUN UNIVERSITY

New metformin derivative HL156A prevents oral cancer progression by inhibiting the IGF/AKT/mTOR pathways

새로운 Metformin 유도체 HL156A가 IGF/AKT/mTOR 경로 저해를 통해 구강암 유도에 미치는 영향 연구

2018년 8월 24일

조선대학교 대학원

치의생명공학과

LAM THUY GIANG

Collection @ chosun

조선대학교
CHOSUN UNIVERSITY

New metformin derivative HL156A prevents oral cancer progression by inhibiting the IGF/AKT/mTOR pathways

지도교수 안 상 건

이 논문을 이학석사학위 신청 논문으로 제출함

2018년 4월

조선대학교 대학원

치의생명공학과

LAM THUY GIANG

Collection @ chosun

조선대학교
CHOSUN UNIVERSITY

LAM THUY GIANG 의 석사학위논문을 인준함

위원장 조선대학교 교 수 방 일 수 (인)

위 원 조선대학교 교 수 유 지 원 (인)

위 원 조선대학교 교 수 안 상 건 (인)

2018년 5월

조선대학교 대학원

Collection @ chosun

조선대학교 CHOSUN UNIVERSITY

ABSTRACT

New metformin derivative HL156A prevents oral cancer progression by inhibiting the IGF/AKT/mTOR pathways

Lam Thuy Giang
Advisor: Prof. Ahn, Sang-gun , PhD
Department of Biodental Engineering,
Graduate School of Chosun University

Metformin, a biguanide widely prescribed as an antidiabetic drug for type 2 diabetes mellitus patients, possesses lately discovered potential anti-cancer properties. The purpose of the present study was to examine the effects of the new metformin derivative, HL156A, on human oral cancer cells and to investigate its possible mechanisms. It was observed that HL156A significantly decreased FaDu and YD-10B cell viability and colony formation in a dose-dependent manner. HL156A also markedly reduced wound closure rate and migration ability of two examining cell lines. We observed that HL156A decreased mitochondrial membrane potential while induced reactive oxygen species (ROS) levels and triggered apoptosis in oral cancer cells with caspase-3 and -9 activation. HL156A inhibited the expression and activation of insulin-like growth factor (IGF)-1 as well as its downstream proteins, AKT, mammalian target of rapamycin (mTOR), and ERK1/2. In addition, HL156A activated AMP-activated protein kinase/ nuclear factor kappa B (AMPK/NF-κB) signaling of FaDu and YD-10B cells. A xenograft mouse model further showed that HL156A suppressed AT84 mouse oral tumor growth, accompanied by down-regulated p-IGF-1, p-mTOR, proliferating cell nuclear antigen (PCNA) and promoted p-AMPK and TUNEL expression. These results suggest the potential value of the new metformin derivative HL156A as a candidate for therapeutic modality of oral cancer.

Collection @ chosun

조선대학교 CHOSUN UNIVERSITY

ABBREVIATIONS

AKT	Protein kinase B
AMPK	5' adenosine monophosphate-activated protein kinase
ANOVA	Analysis of variance
CDK	Cyclin-dependent kinase
CHAPS	3-[(3-cholamidopropyl)dimethylammonio]-1-propanesulfonate
DHE	Dihydroethidium
DTT	Dithiothreitol
EDTA	Ethylenediaminetetraacetic acid
HRP	horseradish peroxidase
PARP	Poly (ADP-ribose) polymerase
ERK	Extracellular signal-regulated protein kinases
FBS	Fetal bovine serum
HEPES	(4-(2-hydroxyethyl)-1-piperazineethanesulfonic acid)
IGF	Insulin-like factor
MMP	Matrix metallopeptidase
mTOR	Mammalian target of rapamycin
MTT	3-(4,5-di methyl thiazol-2-yl)-2,5-diphenyltetrazolium bromide
NFκB	Nuclear factor kappa B
NOS	Nitric oxide synthases
OSCC	Oral squamous cell carcinoma
PBS	Phosphate-buffered saline
PCNA	Proliferating cell nuclear antigen
PI	Propidium iodide
ROS	Reactive oxygen species
RT	Room temperature
SD	Standard deviation
SOD	Superoxide dismutase
TUNEL	Terminal deoxynucleotidyl transferase dUTP nick end labeling

Collection @ chosun

조선대학교 CHOSUN UNIVERSITY

LIST OF FIGURES

Collection @ chosun

조선대학교 CHOSUN UNIVERSITY

Collection @ chosun

조선대학교 CHOSUN UNIVERSITY

TABLE OF CONTENTS

Collection @ chosun

조선대학교 CHOSUN UNIVERSITY

I. INTRODUCTION

Oral squamous cell carcinoma (OSCC), one of the top 10 most commonly occurring cancers worldwide, has a high mortality rate. In spite of recent improvements and advances in medicine such as surgery, radiation, and chemotherapy, the 5-year survival rate for oral cancer patients has remained at 50% over the past 5 decades [1-2] Several clinical applications of surgery, radiation, and chemotherapy are standard treatments for early OSCC, which result in effective tumor control. However, many severe side-effects and/or toxicity appear in patients receiving those treatments [3]. With the unceasingly increasing number cases, the demand of finding new alternative therapeutic strategy for oral cancer is more essential than ever.

Recently, metformin (N, N-dimethylbiguanide) has captured the attention of scientists because of its potential for cancer therapy, although it is primarily widely used as an effective type 2 diabetes medication [4]. Preclinical and clinical studies have shown that metformin significantly prevents cancer incidence, slows tumor progression and improves survival rates with certain types of malignancies including breast cancer, prostate cancer, and salivary adenocarcinoma [5-10]. Among the possible underlying mechanisms of metformin, AMP-activated protein kinase (AMPK) activation is considered one of the most important because AMPK can interact with several other signaling pathways and transcription factors, such as AKT, nuclear factor kappa B (NF-κB), and mammalian target of rapamycin (mTOR) [11-13]. However, the precise mechanism for the multiple anticancer effects of metformin still remains to be elucidated.

Collection @ chosun

조선대학교 CHOSUN UNIVERSITY

Additionally, despite possessing many outstanding properties, limited cell penetration capacity as a result of its hydrophilic nature makes metformin unable to meet the criterions for extensively use as an anticancer drug [11].

HL156A (N-[N-{4-(trifluoromethoxy) phenyl} carbamimidoyl] pyrrolidine-1-carboximidamide acetate) (Figure 1) is a derivative of metformin synthesized from pyrrolidine that is capable of inducing AMPK activation [14]. HL156A have been comfirmed to have high bioavailability since it enters the cell independent of OCT1 (a target transporter of metformin) and penetrates extensively into the brain [16]. It was reported that HL156A has protective effects against peritoneal and liver fibrosis [14-15]. It was also reported that HL156A inhibited LPS-induced inflammation of macrophages. In addition, HL156A inhibits not only smad3-dependent signaling activated by high glucose conditions but also epithelial-mesenchymal transition (EMT) [15]. A recent study showed that HL156A in combination with temozolomide inhibited the invasive properties of glioblastoma and increased the survival rate in a xenograft in vivo model [16]. Given that its structure contains the central biguanide moiety of metformin with improved bioavailability, there are expectations that HL156A may exhibit comparable anticancer properties.

In the present study, the effects of HL156A on the progression of oral cancer cells were examined. The results suggest the potential abilities of the new metformin derivative HL156A as a candidate for a therapeutic modality for oral cancer.

Collection @ chosun

조선대학교
CHOSUN UNIVERSITY

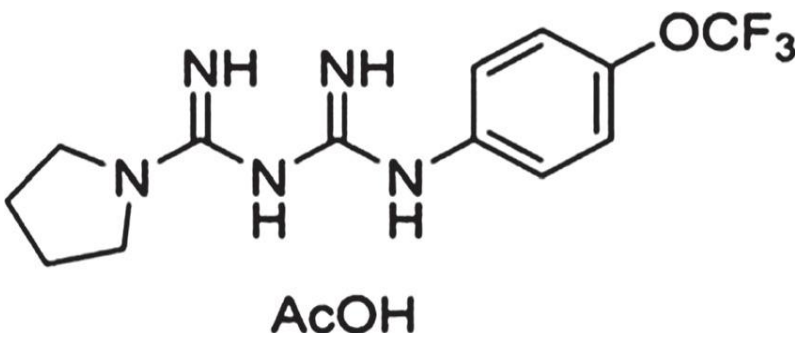

Figure 1. Structure of HL156A

Collection @ chosun

조선대학교 CHOSUN UNIVERSITY

II. MATERIAL AND METHODS

2.1. Cell culture and reagents

For OSCC cell lines, FaDu, YD-10B, and AT84 cells were purchased from Korea Cell Line Bank (KCLB, Seoul, Korea). Human hypopharyngeal squamous cell carcinoma (FaDu) cells were maintained in a complete DMEM (Welgene Inc., Gyeongsanbuk-do, Korea), containing 10% FBS, 100 units/mL penicillin and 100 μg/mL streptomycin. Human oral squamous cell carcinoma (YD-10B) and mouse oral squamous cell carcinoma (AT84) cells were cultured in RPMI-1640 medium containing 10% FBS, 100 U/mL penicillin, and 100 μg/mL streptomycin. The cells were maintained at 37° C in a humidified 5% CO2/95% air atmosphere.

HL156A is a derivative of phenyl biguanide, which is designed and synthesized by Hanall Biopharma Inc. (Seoul, Korea). The detailed procedure of HL156A synthesis was described in previous studies (15-16).

2.2. Cell proliferation assay

Cell proliferation was assessed using an MTT assay. Briefly, cells were seeded in a 96-well plate at a density of $2x10^3$ cells/well. 24 hours post seeding, cells were treated with different concentrations of HL156A (10-50 μmol/L) and incubate at 37° C in a humidified 5% CO2/95% air atmosphere for 24 hours. After incubation, the cells were washed twice with PBS, and 500 μg/mL MTT (Sigma-Aldrich, St Louis, MO, USA) was added to the wells. After 4 hours of incubation at 37° C, the MTT solution was removed and cells were washed once with PBS. A mixture of 40μM HCl in isopropanol was added to each well. Absorbance was measured at 540 nm using a DTX 880 Multimode Detector (Beckman

Collection @ chosun

조선대학교 CHOSUN UNIVERSITY

Coulter, Brea, CA, USA).

2.3. Soft agar colony formation assay

Briefly, cells ($1x10^4$ cells) were exposed to different concentrations of HL156A in 1 mL of 0.3% basal medium Eagle's agar containing 10% FBS and were plated in 60-mm plates containing 0.5% low-melting temperature agarose. The cells were allowed to form colonies for 14 days at 37° C in a humidified atmosphere containing 5% C02. The colonies were fixed with 4% paraformaldehyde for 15 minutes at room temperature and were then stained with 0.05% crystal violet (in 25% Methanol) for 30 min at room temperature. The cell colonies were scored using an IX2-SLP inverted microscope (Olympus, Tokyo, Japan).

2.4. Annexin V-FITC/propidium iodide (PI) double staining and cell cycle analysis

Cell cycle distribution was analyzed using flow cytometry. Briefly, $1x10^6$ cells were harvested, washed in PBS and then fixed in 70% alcohol for 30 min at 4° C. After 3 washes in cold PBS, the cells were resuspended in 1 mL PBS solution containing 50 μL of 1 mg/mL PI and 1 unit DNase-free RNase for 30 min at 37° C. The samples were then analyzed to determine the DNA content using a FACScan analyzer (Beckman Coulter Inc., Fullerton, CA, USA). For cell death analysis,

Annexin V-FITC/PI staining was carried out to examining cell apoptosis based on manufacturer's protocol. Briefly, cell were harvested and washed with PBS once. 100μl of 1X annexin-binding buffer (10 mmol/L HEPES, 140 mmol/L NaCl, 2.5 mmol/L CaCl2, pH 7.4)(Thermo Fisher Scientific, Massachusetts, USA) was

Collection @ chosun

조선대학교 CHOSUN UNIVERSITY

added to resuspend cells. 5μl of Annexin V-FITC (Thermo Fisher Scientific, Massachusetts, USA) and 1μl of 100μg/ml PI(Thermo Fisher Scientific, Massachusetts, USA) working solution were added to each 100μl cell suspension and incubated for 15 min at room temperature (RT). After the incubation period, 400μl of 1X annexin-binding buffer was added to each sample and gently mixed. Stained cells were analyzed by flow cytometry, measuring the fluorescence emission at 530 nm and >575 nm in a FACScan analyzer (Beckman Coulter Inc., Fullerton, CA, USA).

2.5. Western blot analysis

Total protein from the cells was obtained using RIPA buffer (50 mmol/L Tris-Cl (pH 7.5), 150 mmol/L NaCl, 0.5% sodium deoxycholate, 1% NP-40, 0.1% SDS and 1 mmol/L EDTA) containing a protease inhibitor cocktail (1 μg/mL aprotinin and leupeptin). Cell lysates (30 μg) were subjected to SDS-PAGE and then transferred to a nitrocellulose membrane (Amersham Pharmacia Biotech, Buckinghamshire, UK). The membranes were blocked with 5% skim milk for 1 hours and incubated with the primary antibodies. Antibodies against pCDK1 (sc101654), Cyclin B1 (sc245), caspase-3 (sc7148), caspase-9 (sc8355), caspase-7 (sc28295), PARP-1 (sc1561), SOD-1 (sc11407), NOS1 (sc5302), Nrf-2 (sc722), p70S6K (sc230), p-p70S6K (sc8416), p-mTOR (sc 101738), NF-κB (sc109), p-NF-κB (sc101752), MMP2 (sc13594), MMP9 (sc6840) were purchased from Santa Cruz Biotechnology (Santa Cruz, CA, USA). The antibody against AMPK (2532S), p-AMPK (2535S), phosphorylated insulin-like growth factor-1 receptor (pIGF-1R) (3024S), AKT (9272S), pAKT (4060S), ERK1/2 (9102S), p-ERK1/2(9101S), and p-GSK-3a/b (8566S)

Collection @ chosun

조선대학교 CHOSUN UNIVERSITY

and the HRP-conjugated secondary antibody were purchased from Cell Signaling Technology (Beverly, MA, USA). After being washed twice, the membranes were incubated with the corresponding secondary antibodies for 1 hour (dilution ratio 1:5000). Protein signals were detected with a Luminescent image analyzer (LAS-1000; Fujifilm, Tokyo, Japan).

2.6. Caspase activity assay

Caspase-3 and -9 activities were assessed using a caspase-3 or -9 colorimetric assay kit (Abcam, Cambridge, MA, USA) according to the manufacturer's protocol. Briefly, the cells were collected and resuspended in lysis buffer containing 50 mmol/L HEPES, pH 7.4, 0.1% CHAPS, 1 mmol/L DTT, 0.1 mmol/L EDTA and 0.1% Triton X-100. Following incubation for 30 min on ice, cell lysate was centrifuged at 11 000 g for 10 min at 4° C, and the protein concentration in the supernatants was measured using the Bradford dye method. The supernatants were incubated with reaction buffer containing 2 mmol/L Ac-DEVD-AFC for caspase-3 and LEHD-AFC for caspase-9 (Abcam) in a caspase assay buffer at 37° C with 10 mmol/L DTT for 30 min. Caspase activity was determined by measuring the absorbance at 405 nm using Beckman Coulter DTX 880 Multimode Detector (Beckman Coulter Inc., Fullerton, CA, USA).

2.7. Mitochondrial membrane potential

Mitochondrial membrane potential was analyzed by flow cytometry using a JC-1 mitochondrial membrane potential detection kit (Biotium Inc., Hayward, CA, USA). JC-1 exhibits potential-dependent accumulation in mitochondria, indicated by a fluorescence emission shift from green (530 nm, FL-1 channel) to red (590

Collection @ chosun

조선대학교 CHOSUN UNIVERSITY

nm, FL-2 channel). After treatment with or without 40 μmol/L HL156A, oral cancer cells were incubated in JC-1 reagent working solution (Biotium Inc., Hayward, CA, USA) for 15 min at 37° C, washed once with PBS and then resuspended in staining buffer and analyzed with a fluorescence microscope (Olympus,Tokyo, Japan).

2.8. Reactive oxygen species formation detection

Determination of reactive oxygen species (ROS) levels was based on the oxidation of dihydroethidium (DHE). Cells were seeded to reach 70%-80% confluency and then incubated with HL156A (5μmol/L or 40μmol/L) for 3, 6, and 12 hours. Cells were then treated with DHE (5 mmol/L) for 30 min at 37° C in the dark. The cells were then washed twice and harvested in PBS. Fluorescence of DHE was detected with a fluorescence microscope (IX-71; Olympus, Tokyo, Japan) at the excitation/emission wavelength 510/595 nm.

2.9. Wound-healing motility assay

Cells were allowed to grow in a culture dish overnight and a scratch (~3 mm wide) was created in the monolayer using a pipette tip. After being washed twice with PBS, the cells were treated with or without HL156A, and images were captured after 24 hours post treatment. Cells were imaged in 5 random microscopic fields per well using an Olympus IX2-SLP inverted microscope (Olympus) at x100 magnification.

2.10. Migration assay

Cell migration was determined using a modified 2-chamber migration assay with a pore size of 8 mm. For the migration assay, cells suspended in 500 μL

Collection @ chosun

조선대학교 CHOSUN UNIVERSITY

serum-free medium were seeded on the upper compartment of a 12-well Transwell culture chamber, and 700 μL complete medium was added to the lower compartment. After incubation at 37° C, migratory cells in the medium in the lower chamber were quantified by measuring the absorbance at optical density (OD) 595 nm.

2.11. In vivo mice xenograft experiments

Mouse oral cancer AT84 cells were treated with or without 20 μmol/L HL156A for 24 hours. Cells (1 x 10^6 cells per mouse) were injected s.c. into the left flank of 3-week-old male C3H mice (Samtaco Bio, Sungnam, Korea) in each group (n = 5 or 7). Bodyweight was measured every 2 days during the experiment. Three weeks later, tumor volume was measured with a caliper and calculated using the formula V = (ab2)/2, where a was the longest diameter and b was the shortest diameter of the tumor. All mice were sacrificed on day 21, and the tumors were removed, weighed, and subjected to further analysis. Formalin-fixed paraffin-embedded tissues from AT84 xenografted tumors were used for immunohistochemical staining of p-IGF-1, p-mTOR, p-AMPK, and PCNA expression.

2.12. Statistical analysis

All experiments were carried out at least in triplicate. Results are expressed as the mean _ standard deviation (SD). Student's t test and one-way analysis of variance (ANOVA) were used to determine the significant difference between the control and experimental groups. P-values less than 0.05 were considered statistically significant.

Collection @ chosun

조선대학교 CHOSUN UNIVERSITY

III. RESULTS

3.1. HL156A suppresses oral cancer cell growth

To investigate the effects of HL156A on oral cancer cell proliferation, MTT assays were carried out with different concentrations (10 to 50 μmol/L) of HL156A in FaDu and YD-10B cells. HL156A significantly decreased the growth of FaDu cells in a concentration-dependent manner (Figure 2A). In FaDu cells, 40 μmol/L HL156A resulted in cell growth inhibition rates of 45% at 24 hours. Similarly, cell growth inhibition in YD-10B cells was also observed with HL156A treatment (Figure 2B).

To further confirm the effect of HL156A on cell proliferation, a soft agar colony formation assay was carried out. The number of colonies observed was appreciably reduced compared with the control untreated FaDu and YD-10B cells (Figure 2C). Moreover, the size of the colonies was also reduced. At 40 μmol/L, HL156A markedly decreased the clonogenicity to approximately 25% and 13% compared to the control in both cell lines, respectively (Figure 2D). Thus, the results showed that HL156A inhibits the colony-forming ability of oral cancer cells.

Collection @ chosun

조선대학교
CHOSUN UNIVERSITY

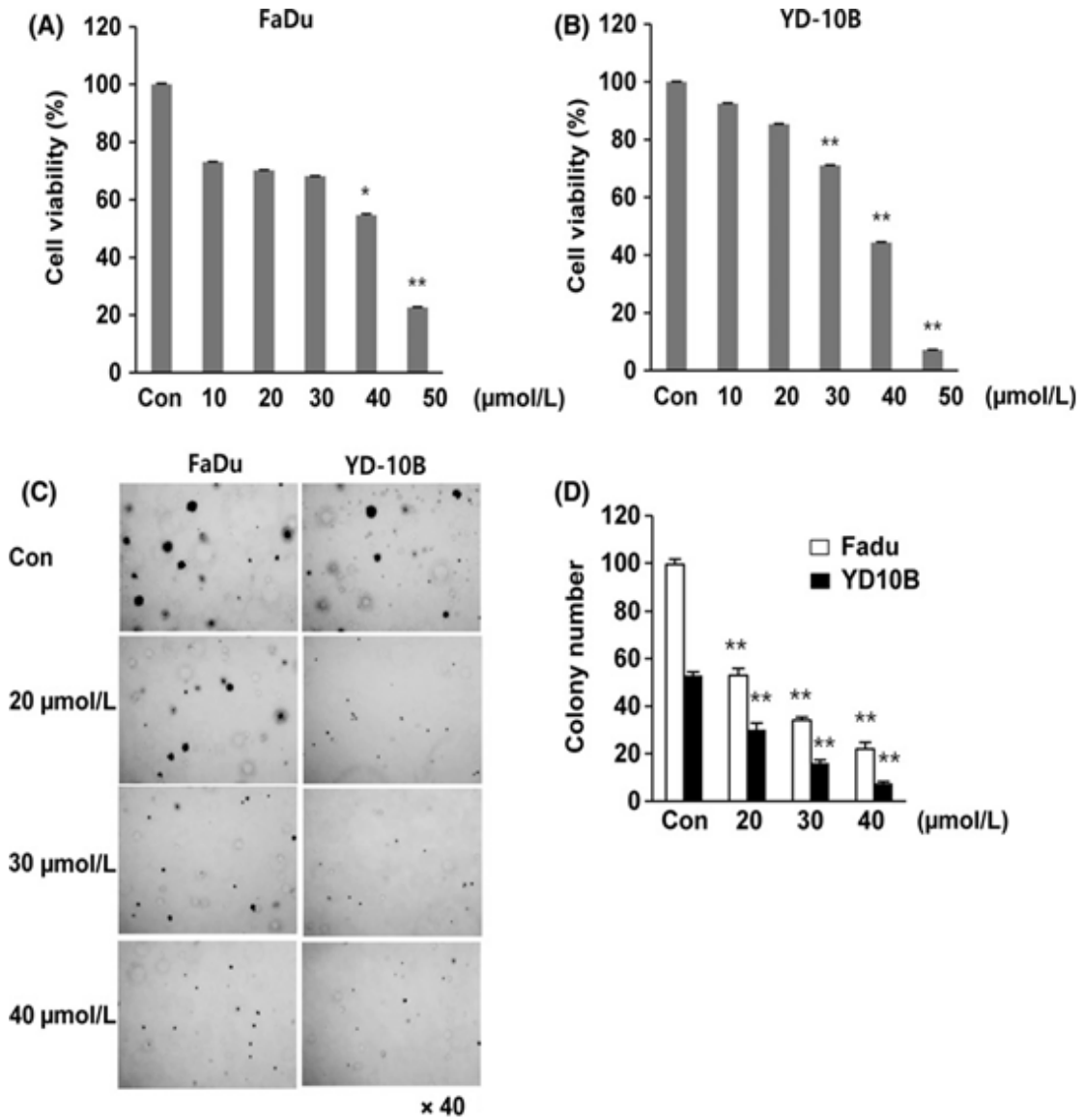

Collection @ chosun

조선대학교 CHOSUN UNIVERSITY

Figure 2. The effect of treatment with HL156A on cell proliferation of oral cancer cell lines.

(A and B) Cell viability was assessed after 24 hours of HL156A treatment at concentrations ranging from 10 to 50 μM in the human oral cancer cell lines FaDu and YD-10B using an MTT assay. The data are expressed as the means ± SD of the results from three separate experiments (*P<0.05 and **P<0.01). (C and D) Evaluation of the colony formation of HL156A-treated cells. Colony formation was assessed 14 days after HL156A treatment at various concentrations, and cells were stained with crystal violet at the end of the experiment. Images were taken with an inverted microscope at ×40 magnification. Colony quantification was determined by microplate area scan at OD 550 nm.

Collection @ chosun

조선대학교 CHOSUN UNIVERSITY

3.2. HL156A induces G2/M cell cycle arrest and cell apoptosis

It was hypothesized that HL156A could induce alterations in cell cycle regulation. Using flow cytometry, we analyzed the effect of HL156A on cell cycle progression. As shown in Figure 3A, HL156A treatment caused a reduction in the G1 phase population and an increase in the G2/M population in both FaDu and YD-10B cells. In YD-10B cells, the percentage of cells in G1 phase decreased from 53% to 5.2% after 60 μmol/L HL156A treatment for 24 hours. The proportion of cells in G0 phase increased from 0.39% to 24.2% over this same interval. In FaDu and YD-10B cells, western blotting analysis showed that the levels of phospho-CDK1 and cyclin B were decreased by HL156A in a time-dependent manner (Figure 3B). These results suggest that the effects of HL156A on G2/M cell cycle progression were associated with the inhibition of cell growth.

To determine whether HL156A induces cell death in FaDu and YD-10B cells, we quantified apoptosis with flow cytometry using an Annexin v-FITC/PI double staining assay. As shown in Figure 4A, 24 hours post-treatment with HL156A (40 or 60 μmol/L), there was a significant decrease in the number of living cells; 93.5% of the control cells were alive, whereas only 60.6% or 6.6% of the HL156A treated FaDu cells were alive, respectively. Moreover, treatment with 40 μmol/L or 60 μmol/L HL156A stimulated a noteworthy increase in the proportion of apoptotic cells (32.9% with 40 μmol/L and 85.3% with 60 μmol/L, respectively) compared to the untreated control. Similarly, a marked number of dying cells were observed in the HL156A-treated YD-10B cells. Consistent with this observation, pro-caspase-3, -7, -9, and the inactive form poly (ADP-ribose)

Collection @ chosun

조선대학교 CHOSUN UNIVERSITY

polymerase (PARP) were decreased in cells treated with HL156A compared with the control in a time-dependent manner (Figure 4B). In addition, caspase-3 and caspase-9 activity was progressively induced by HL156A treatment in a time-dependent manner (Figure 4C, 4D).

Collection @ chosun

조선대학교 CHOSUN UNIVERSITY

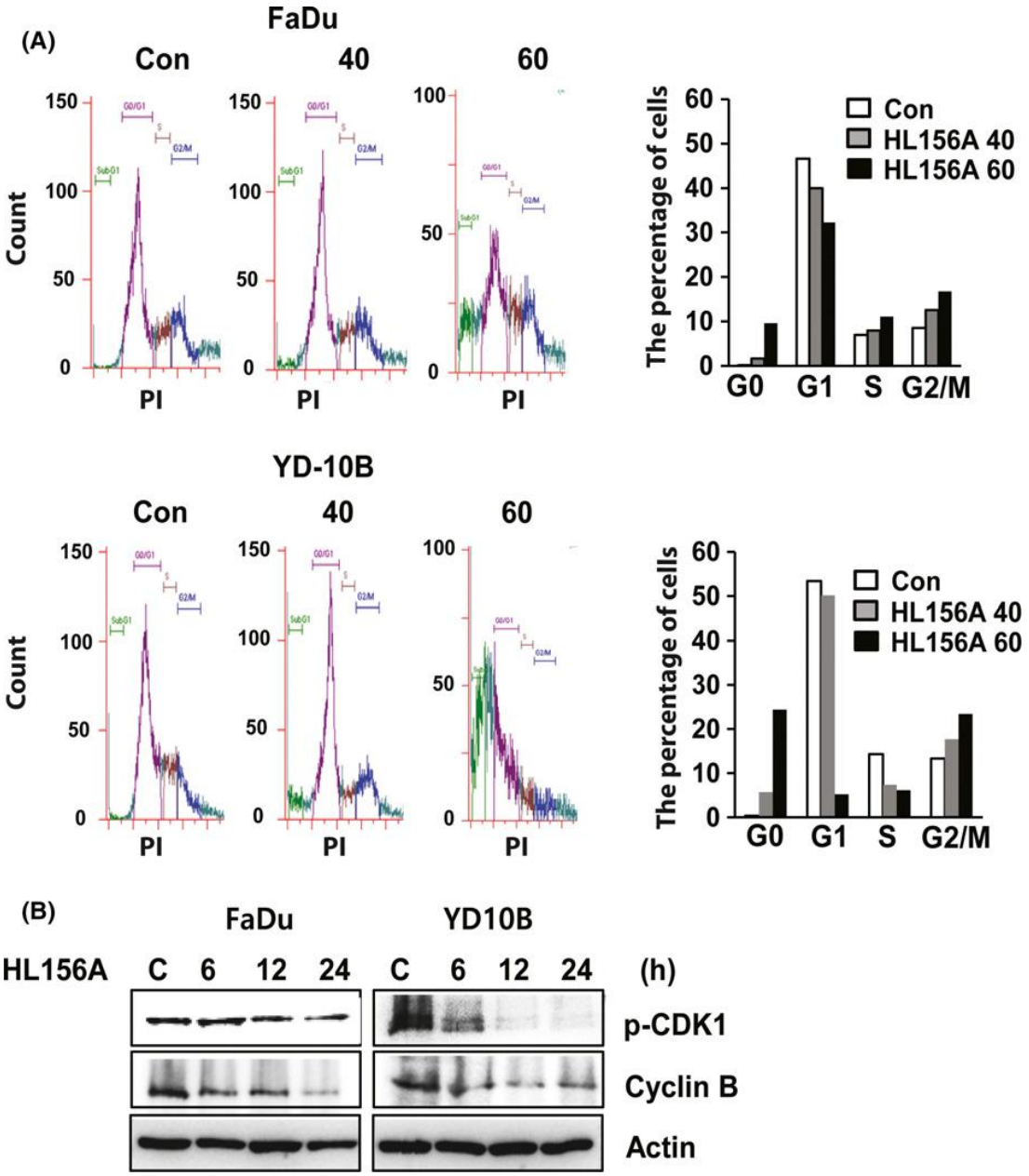

Collection @ chosun

조선대학교 CHOSUN UNIVERSITY

Figure 3. HL156A induces cell cycle arrest at the G2/M phase.

(A) Cells were incubated with HL156A (40μmol/L or 60 μmol/L) for 24 hours and then subjected to flow cytometry to measure cell cycle distribution. The percentage of cells in each cell cycle phase was graphed. (B) Immunoblotting of cell cycle-related proteins in FaDu and YD-10B cells treated with 40 μmol/L HL156A for the indicated times. Lysates of examining cells were subjected to western blotting with phospho-CDK1 and cyclin B antibodies. β-actin served as an internal control.

Collection @ chosun

조선대학교 CHOSUN UNIVERSITY

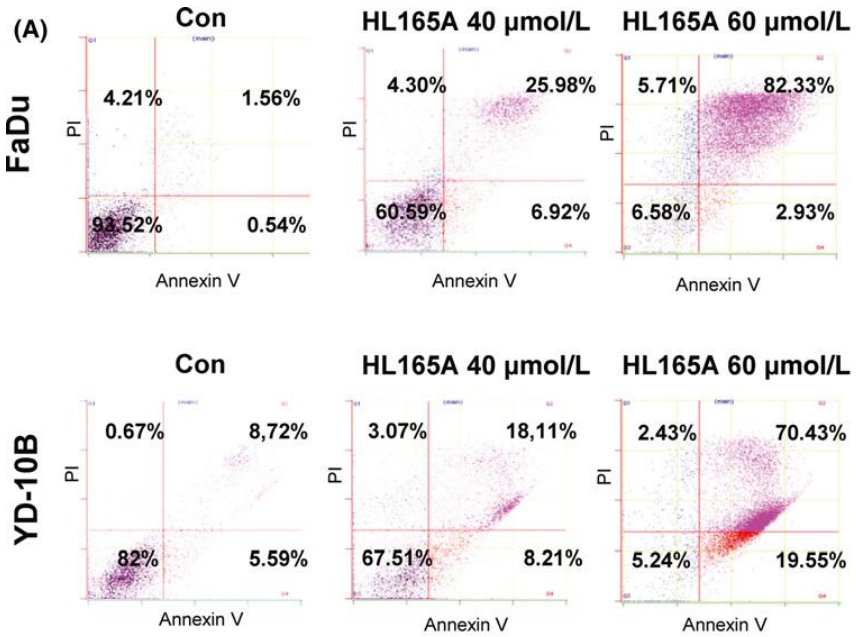

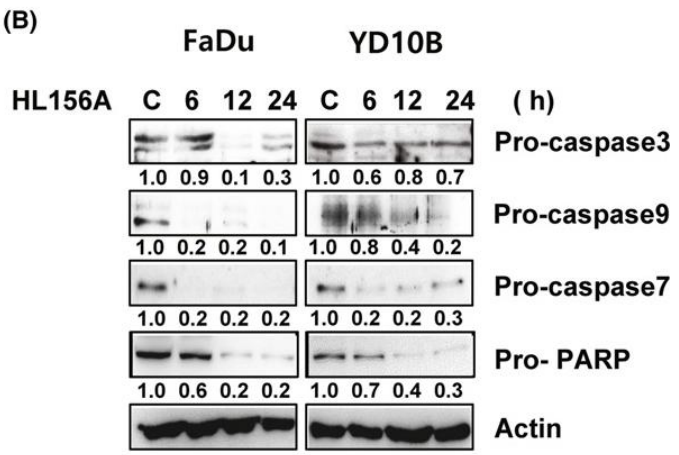

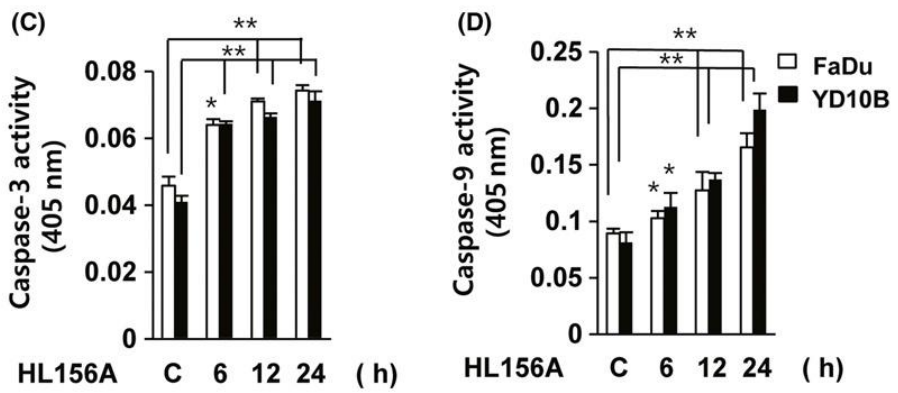

Collection @ chosun

조선대학교 CHOSUN UNIVERSITY

Figure 4. HL156A induces apoptosis in FaDu and YD-10B cells.

(A) Cells were incubated with HL156A (40 μmol/L or 60 μmol/L) for 24 hours. Annexin v-positive apoptotic cells were assessed via flow cytometric analysis after staining with Annexin V/PI. (B) The effect of HL156A on the activity of caspase 3, 7, and 9 and PARP. The cells were treated with HL156A, and cell lysates were subjected to western blotting using antibodies against pro-caspase 3, 7, and 9 and PARP. (C and D) FaDu and YD-10B cells were treated with HL156A (40 μmol/L) for the indicated times and assayed for caspase 3 and caspase 9 activity as described in Materials and Methods.

Collection @ chosun

조선대학교 CHOSUN UNIVERSITY

3.3. HL156A reduces mitochondrial membrane potential and promotes ROS formation

Loss of mitochondrial membrane potential can lead to the release of apoptotic-inducing factors and caspase activators, such as cytochrome c [17]. To determine the changes in mitochondrial membrane potential after exposure to HL156A, cells were assessed using a Mitochondrial Membrane Potential Assay (Biotium Inc., Hayward, CA, USA) with JC-1. JC-1 is a fluorescent cationic dye that can selectively enter into mitochondria and reversibly change color from red to green as the membrane potential decreases. Interestingly, green fluorescence was increased in HL156A-treated cells, suggesting that HL156A led to a reduction in membrane potential (Figure 5A).

To further explore the link between ROS formation and the antiproliferative effects of HL156A, expression of antioxidant proteins was examined. Treatment with HL156A inhibited the level of SOD-1 and NOS in both cells in a time-dependent way (Figure 5B). However, the expression of Nrf-2 and its downstream target HO-1 was not changed during treatment with HL156A. It has been reported that mitochondrial malfunction leads to accumulation of ROS [18]. Intracellular ROS production was assessed with fluorescence microscopy using the oxidation-sensitive dye DHE. The results showed that, in FaDu and YD-10B cells, the level of ROS was time- and/or dose- dependently increased upon treatment with HL156A, suggesting that ROS play a significant role in HL156A-mediated antiproliferation and/or apoptosis (Figure 5C, 5D).

Collection @ chosun

조선대학교 CHOSUN UNIVERSITY

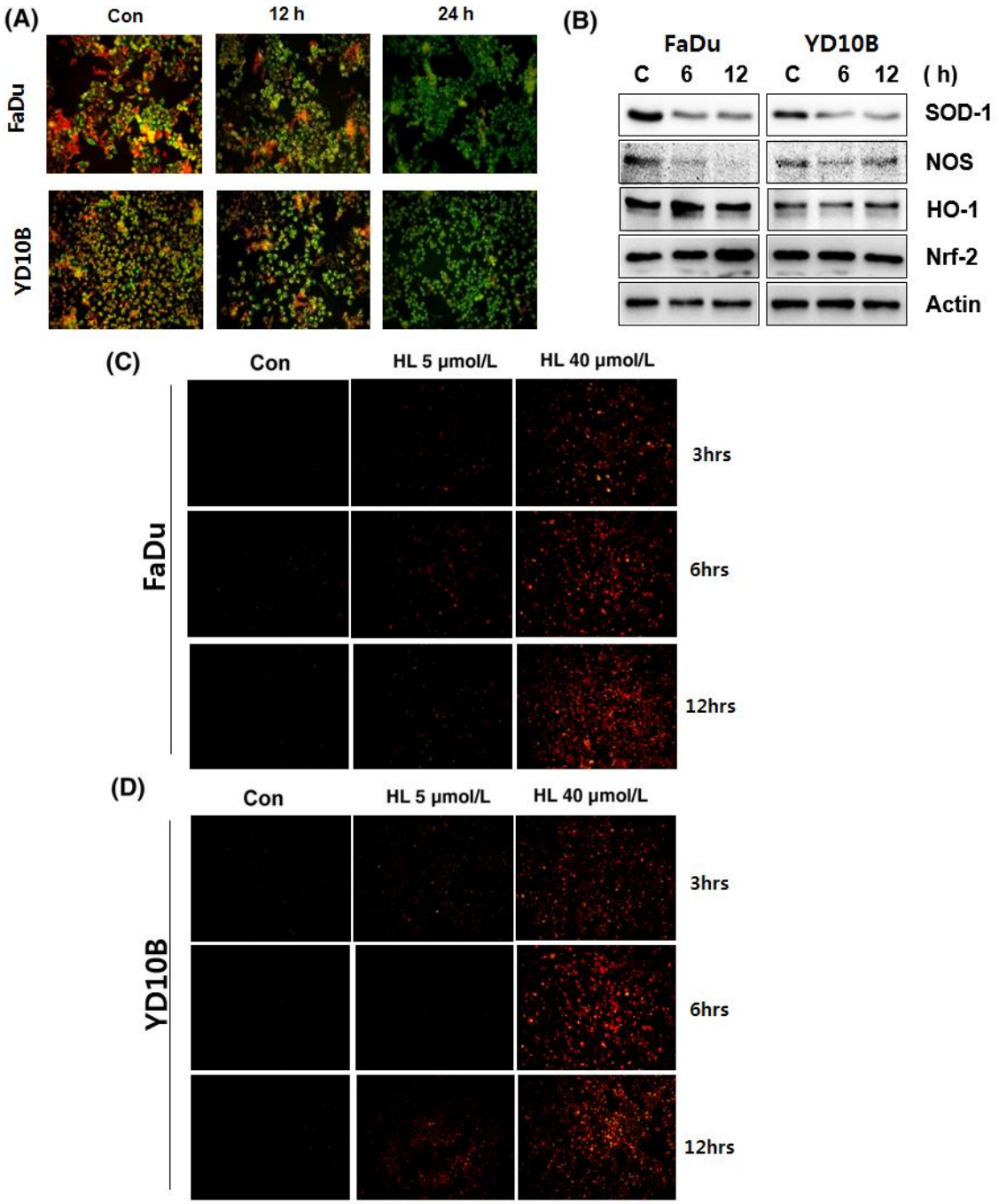

Collection @ chosun

조선대학교 CHOSUN UNIVERSITY

Figure 5. Mitochondrial membrane potential and ROS production in cells treated with HL156A.

(A) FaDu and YD-10B cells were treated with 40 μM HL156A for 12 or 24 hours. Changes in mitochondrial membrane potential were monitored by loading cells with the fluorescent probe JC-1 followed by analysis with fluorescence microscopy. (B) The effect of HL156A on SOD-1 and Nrf/HO-1 expression. FaDu and YD-10B cells were treated with HL156A for the indicated times. Total cell lysates were immunoblotted with antibodies against SOD-1, NOS, Nrf-2, and HO-1. (C and D) ROS were measured in FaDu and YD-10B cells treated with HL156A (5 or 40 μmol/L) for 3, 6, and 12 hours. Cells were loaded with DHE (5 mmol/L) and viewed using fluorescence microscopy.

Collection @ chosun

조선대학교 CHOSUN UNIVERSITY

3.4. Effects of HL156A on insulin- and AMPK signaling pathways

To investigate the molecular mechanisms underlying the effects of HL156A on oral cancer cells, we focused attention on the insulin-like growth factor (IGF)/AKT/mTOR and AMPK pathways since previous studies have revealed that metformin exerts anti-tumor effect through the inhibition of PI3K/AKT/mTOR signaling and the activation of AMPK signaling [12].

Phospho-IGF-1 levels decreased significantly after 12 hours incubation in the presence of HL156A in FaDu and YD-10B cells (Figure 6A). It is observed that HL156A treatment inhibited AKT and ERK phosphorylation/activation and repressed phosphorylation of mTOR and p70S6K in a time-dependent way. The results indicated that HL156A could suppress activation and/or expression of IGF-I, leading to repression of phosphorylation of AKT and mTOR, which subsequently repressed phosphorylation of p70S6K. HL156A also inhibited AKT/ERK1/2 signal transduction pathways that are important for cell proliferation as shown by a decrease in the expression of p-ERK1/2 (Thr202/Tyr204) after 6 hours of treatment (Figure 6A). Furthermore, western blot results showed that p-AMPK was increased in HL156A-treated FaDu and YD-10B cells whereas total AMPK remained unaltered (Figure 6B). AMPK is involved in the expression of inflammatory cytokines through NF-κB [19]. Therefore, we examined the expression of NF-κB subunit p65 (NF-κB p65) in both types of cells treated with HL156A for 6 to 24 hours. HL156A decreased the expression of phosphorylated NF-κB-p65 in FaDu and YD-10B cells in a time-dependent manner.

Collection @ chosun

조선대학교 CHOSUN UNIVERSITY

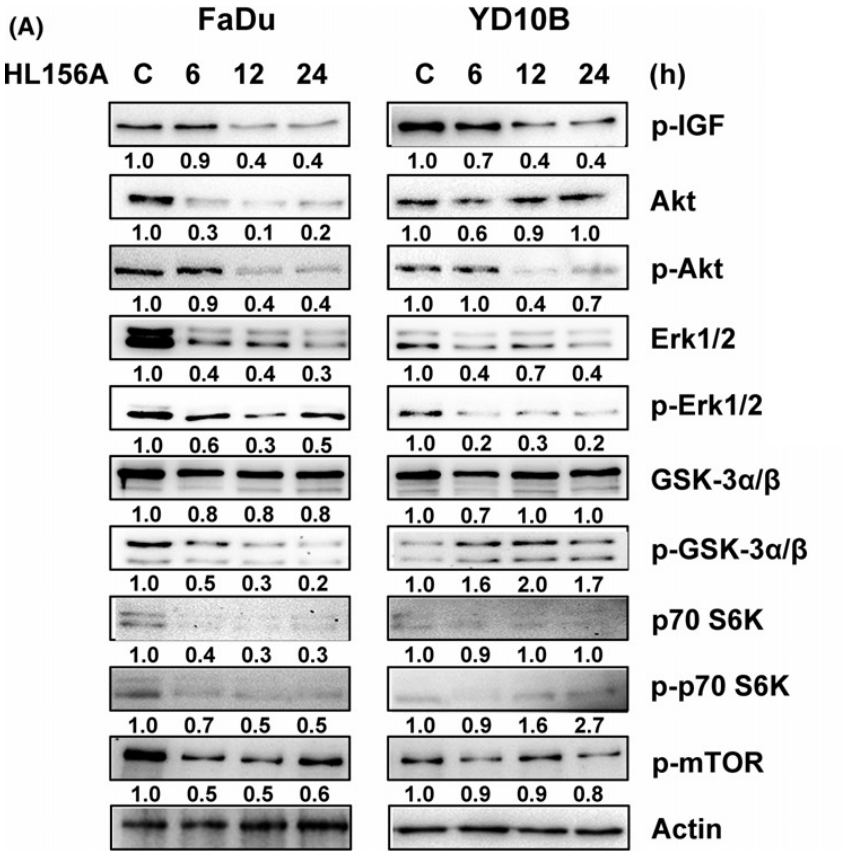

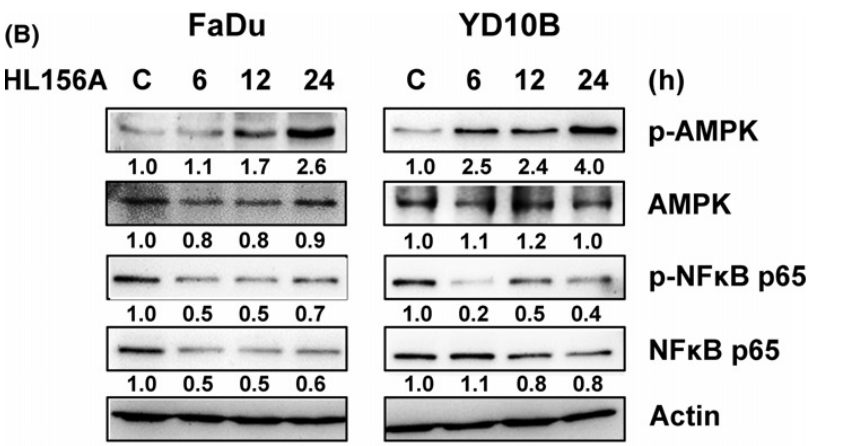

Collection @ chosun

조선대학교 CHOSUN UNIVERSITY

Figure 6. HL156A regulates the insulin-like growth factor (IGF)/AKT/mammalian target of rapamycin (mTOR) pathway and AMP-activated protein kinase/nuclear factor kappa B (AMPK/NF-κB) signaling in FaDu and YD-10B cells.

(A) Cells were treated with HL156A (40 μmol/L) for the indicated times, and the total protein was subjected to western blotting analysis using antibodies against IGF-1R, AKT, mTOR, p70S6K, ERK1/2, and GSK-3. (B) Expression and activation of AMPK and NF-κB were detected with western blotting. Numbers represent relative density normalized to actin.

Collection @ chosun

조선대학교 CHOSUN UNIVERSITY

3.5. HL156A decreases the migration capacity

Metastasis is one of the most important features of cancer. Therefore, to test whether HL156A modulates cell motility, we performed a wound-healing experiment. Restoration of FaDu and YD-10B cells treated with 40μM HL156A slowly closed the scratch wound compared with the control cells at 24 h after initiation of the scratch (Figure 7A).

To confirm whether HL156A inhibits cell migration, we performed *in vitro* Matrigel Transwell chamber assays. When the FaDu and YD-10B cells were treated with HL156A, cell migration was significantly inhibited. HL156A, at a concentration of 40 μmol/L, decreased the migration of FaDu and YD-10B cells to 85% and 70% that of the control cells after 24 h of treatment (Figure 7B).

Several studies have indicated that MMP signaling pathways play an important role in tumor invasion and migration [17-18]. To elucidate the mechanism by which HL156A inhibits migration in FaDu and YD-10B cells, we monitored the expression of MMP2 and MMP9. The levels of MMP2 and MMP9 were reduced by HL156A treatment in a time-dependent manner; with 50% inhibition in 40 μmol/L HL156A-treated FaDu and YD-10B cells (Figure 7C).

Collection @ chosun

조선대학교 CHOSUN UNIVERSITY

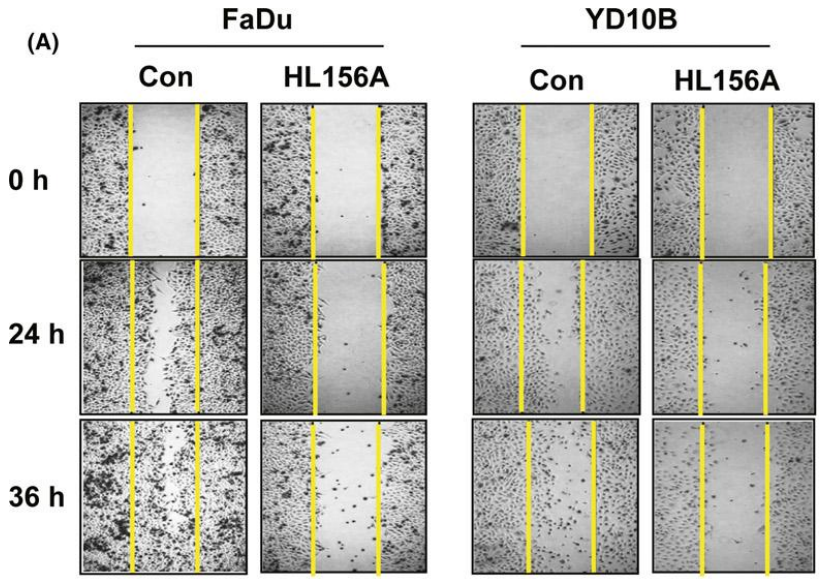

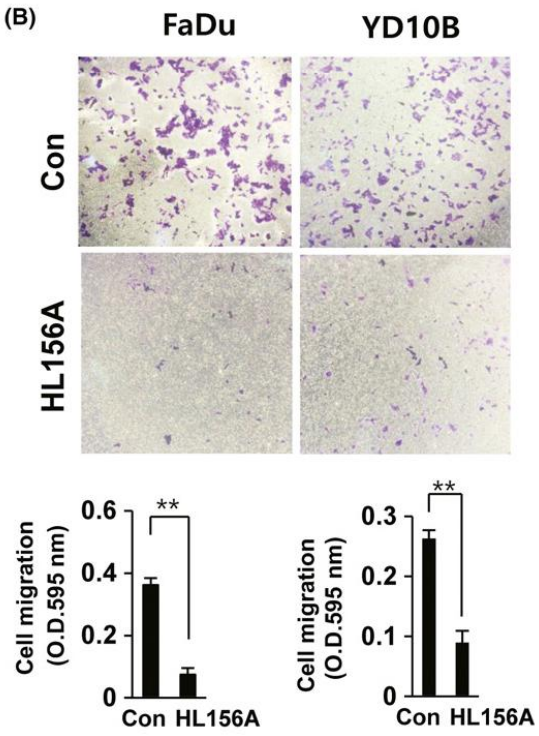

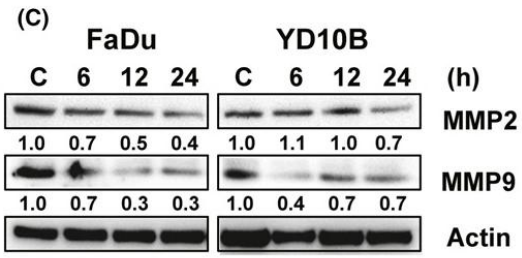

Collection @ chosun

조선대학교 CHOSUN UNIVERSITY

Figure 7. HL156A inhibits cell migration and MMP2 and MMP9 expression.

(A) A wound-healing assay showed the closure rates of cells treated with HL156A. Images of wound-closure rates at the indicated time-points. (B) The effect of HL156A on cell migration. Cells were treated with 40 μmol/L HL156A for 24 h. Migration assays were performed as described in the Materials and Methods section. The graphs show the quantitative evaluation of the migration rates. The results represent the averages of three independent experiments. (C) The expression of MMP2 and MMP9 in HL156A-treated cells. FaDu and YD-10B cells were treated with HL156A (μmol/L) for the indicated times and subjected to western blotting.

Collection @ chosun

조선대학교 CHOSUN UNIVERSITY

3.6. HL156A suppresses tumor growth in a xenograft mouse model

In support of the identified in vitro anti-proliferative effects of HL156A, a tumor xenograft model was used to examine alterations in the pathological characteristics in vivo. C3H mice were randomized and s.c. engrafted with mouse oral cancer AT84 cells treated in vitro with or without HL156A (20 μmol/L). As shown in Figure 8, HL156A significantly inhibited tumor growth up to 82% relative to the control group at the end of the experiment (21 days). No systemic toxicity, including bodyweight changes, or other apparent adverse effects were observed in the animals throughout the study period (Figure 8A).

Histological differences between the HL156A treated and control groups were examined using H&E staining. Tumor tissues treated with HL156A had larger areas of extensive cell changes showing nuclear pyknosis and cytoplasmic eosinophilia. In immunohistochemistry assay, tumors from the HL156A-treated group showed decreased levels of phosphorylated IGF-1 and mTOR compared to control. Consistent with our western blot findings, HL156A increased the expression of p-AMPK compared with control (Figure 8C). The antitumoral effects of HL156A in the in vivo study were also investigated by examining the expression of PCNA, a cell proliferation marker, and by TUNEL staining to assess the number of apoptotic cells using immunohistochemistry. The number of PCNA-positive cells was significantly decreased in HL156A-treated tumor sections compared with tumors from control mice. The number of TUNEL-positive cells was dramatically increased in HL156A-treated tumor tissues, suggesting that the

Collection @ chosun

조선대학교 CHOSUN UNIVERSITY

effect of HL156A on inhibition of tumor growth and the induction of apoptotic cell death is consistent with the antitumor activity of HL156A *in vitro*.

Collection @ chosun

조선대학교
CHOSUN UNIVERSITY

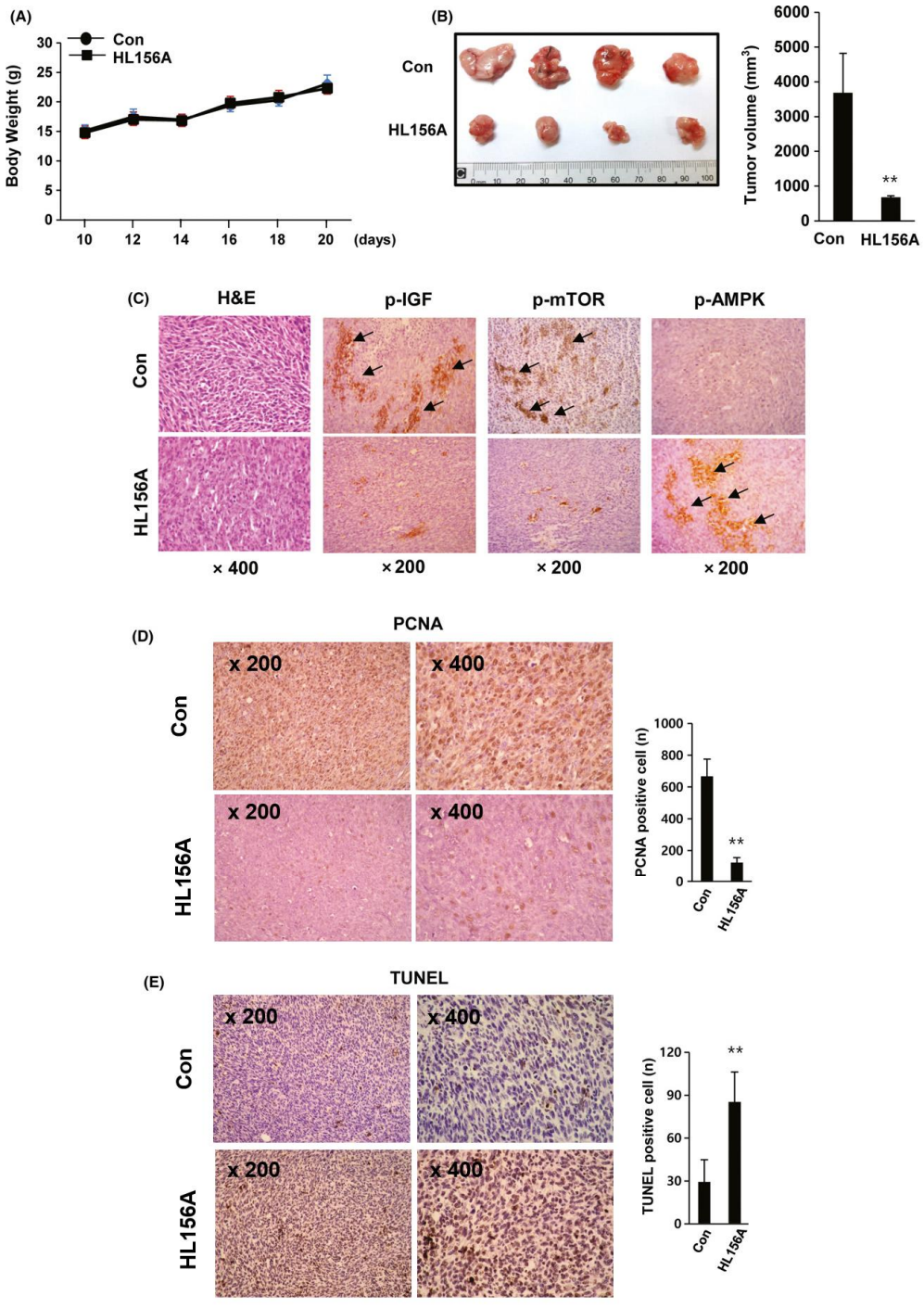

Collection @ chosun

조선대학교 CHOSUN UNIVERSITY

Figure 8. HL156A inhibits tumor growth in a mouse AT84 xenograft model.

(A,B) Inhibition of tumor growth. Mouse oral cancer AT84 cells ($1x10^6$ cells/mouse) treated with 20 μmol/L HL156A were injected s.c. into the left flanks of male C3H mice (n = 7 per group). Tumor growth was assessed by monitoring the mass volume 2 times a week. Bodyweight was monitored and plotted against time for the HL156A (closed squares) and control groups (closed circles). Tumor volume was measured at 20 days and calculated using the formula $V = (ab^2)/2$ where a was the largest diameter and b was the shortest diameter of the tumor. **P < 0.01 compared to untreated control. (C-E) Immunohistochemistry of tumor sections. Immunohistochemistry for phosphorylated insulin-like growth factor (p-IGF), phosphorylated mammalian target of rapamycin (p-mTOR), AMP-activated protein kinase (AMPK), proliferating cell nuclear antigen (PCNA) or TUNEL was carried out on paraffin-embedded tumor sections. Graphs show the quantitative evaluation of the number of PCNA- or TUNEL-positive cells.

Collection @ chosun

조선대학교 CHOSUN UNIVERSITY

IV. DISCUSSION AND CONCLUSION

Previous studies suggest that metformin inhibits the proliferation and growth of various types of cancer [3,22-24]. In addition, metformin is also associated with decreased incidence of breast, liver, pancreatic, and colorectal cancers in diabetic patients [6,7,11,12]. However, the pathways that contribute to the anticancer effects of metformin have still not been elucidated. Currently, researchers want to know whether metformin or its derivatives may have additional uses in other diseases, including cancer. Although metformin contributes to the anticancer effects, delivery of metformin to the tissue is limited. Specifically, metformin has limitations as an anticancer drug because its hydrophilic nature prevents it from entering cells [25]. HL156A overcomes this shortcoming and shows generally high bioavailability. For example, the prominent survival benefit of in vivo combination treatment with HL156A may be attributable to the excellent penetration ability of HL156A [16]. In addition, a number of studies have shown the specific effect of metformin on various human cancers. High concentrations of metformin (up to 10-15 mmol/L) have been shown to inhibit proliferation of various human cancer cell lines such as lung cancer cells (up to 15 mmol/L), endometrial cancer cells (up to 10 mmol/L), hepatocellular carcinoma cells (up to 10 mmol/L), and head and neck squamous carcinoma cells (5-20 mmol/L) [26-28]. HL156A exerted more potent inhibitory effects on the proliferation of glioblastoma cells than metformin. HL156A showed approximately 100-fold more potent effects compared to metformin. In a glioblastoma xenograft model, HL156A showed a comparable degree of inhibitory

Collection @ chosun

조선대학교 CHOSUN UNIVERSITY

effect on in vivo tumor growth at the 30 mg/kg dose to that of metformin at 100 mg/kg [16,29]. We also found that HL156A inhibits cell growth at lower concentrations (≤40 μmol/L) than metformin in oral squamous carcinoma cells.

In this study, it is observed that the new metformin derivative HL156A significantly reduced growth of human oral squamous cell carcinoma FaDu and YD-10B cells. HL156A treatment led to a reduction in colony formation in a dose-dependent manner. Moreover, the inhibitory properties of HL156A observed were markedly augmented when HL156A was used to treat oral cancer cells, even with a dose as low as 40 μmol/L. The cell cycle was inhibited at the G2/M phase in the HL156A-treated cells that were analyzed. Consistent with these results, HL156A treatment led to a remarkable decrease in cyclin B and cyclin-dependent kinase (CDK) 1 activity in FaDu and YD-10B cells. These results suggested that the effects of HL156A on cell cycle progression were associated with inhibition of cell growth and cell death induction.

Interestingly, we first found that HL156A-mediated apoptotic cell death was possibly associated with promotion of intracellular oxidative stress. Consistent with previous reports regarding the relationship between the anticancer potency of metformin and the generation of ROS [30]. The results showed that treatment with HL156A led to a reduction in mitochondrial membrane potential as well as an increase in ROS production in a time- and dose-dependent manner. Furthermore, mitochondrial antioxidant proteins, such as SOD-1 and NOS, were also down-regulated, but not the Nrf/Ho-1 pathway. The imbalance between excessive ROS production and SOD-1 depletion may cause oxidative stress for oral

Collection @ chosun

조선대학교 CHOSUN UNIVERSITY

cancer cells. This, combined with the reduction in membrane potential, resulted in the release of pro-apoptotic factors, such as cytochrome c, and the stimulation of caspases, which ultimately ends in apoptosis [17]. Our study showed that HL156A gradually increased cell apoptosis, as evidenced by the increased activity of caspase-3, -7, -9, and poly (ADPribose) polymerase (PARP).

Another important point is that HL156A exerted more potent inhibitory effects on the migration of oral cancer cells than metformin. Wound healing assays and migration assays showed invasion and/or migration properties of HL156A. Downregulation of MMP-2 and MMP-9 protein levels were also detected in a time-dependent manner following HL156A treatment. Previous studies showed that anticancer drugs markedly suppressed migration and invasion in malignant cancer cells and HUVEC, and the effect was partially MMP-dependent [20,21,31]. Our results indicated that HL156A is involved in the inhibition of FaDu and YD-10B cell migration through their ability to breakdown the extracellular matrix, especially MMP-2 and MMP-9.

Recent studies proved that IGF-1 activates two main downstream signaling pathways, the PI3K/AKT/mTOR and the Ras-Raf-MEK/ERK pathways [32]. Activation of the PI3K/AKT/mTOR pathway is known to promote cell proliferation and cell cycle progression and to reduce apoptosis, which ultimately leads to a competitive growth advantage, metastatic competence, angiogenesis, and therapy resistance [33,34]. AKT can directly phosphorylate and activate mTOR. mTOR plays a major role in carcinogenesis, and activation of this pathway is associated with cancer progression [34]. In the present study, HL156A was involved in mediating the

Collection @ chosun

조선대학교 CHOSUN UNIVERSITY

antiproliferation effect through inhibiting the IGF/AKT/mTOR/p70S6K pathway in FaDu and YD-10B cells. In addition, HL156A blocked the phosphorylation of the AKT substrate glycogen synthase kinase 3b and ERK1/2. A previous study showed that suppression of AKT/ERK signaling resulted in apoptosis, indicating that the activation of AKT/ERK promoted survival under cellular stress [35]. Collectively, these results strongly suggested that IGF/AKT/mTOR and AKT/ERK pathways play an important role in maintaining the viability of oral cancer cells. Our results implied that the effects of HL156A were partially induced by inhibiting these pathways, IGF/AKT/mTOR and/or AKT/ERK.

Herein, it is also confirmed that HL156A importantly induced activation of AMPK by phosphorylation together with suppression of NFκB p65 in FaDu and YD-10B cells. A number of studies have shown indirect suppression of AMPK on NF-κB signaling by its downstream mediators, namely SIRT1, the Forkhead box O (FoxO) family, and peroxisome proliferator-activated receptor c co-activator 1a (PGC-1a) [36]. The HL156A-mediated decrease in NF-κB p65 phosphorylation may be accompanied by AMPK activation. These results may suggest a role for HL156A in inhibiting the activation of NF-κB as well as in inhibition of the expression of proteins/cytokines that regulate inflammation. The importance of these signaling pathways in the pathogenesis of cancer development is suggested from a number of studies.

A recent research revealed that HL156A in combination with the chemotherapeutic agent temozolomide (TMZ) inhibited the invasive properties of glioblastoma and increased the survival rate in a xenograft mouse model [13].

Collection @ chosun

조선대학교 CHOSUN UNIVERSITY

In this study, consistent with that finding, HL156A significantly reduced the growth of mouse oral squamous cell carcinoma AT84 xenograft tumors. In the immunohistochemistry assay, the number of proliferative cells was dramatically decreased, whereas the number of apoptotic cells was considerably increased. Importantly, p-IGF-1 and p-mTOR expression were weak in control group tissues compared with HL156A-treated tumor tissues. In contrast, p-AMPK expression was stronger in HL156A-treated tumor tissues. Overall, our results indicated that induction of apoptosis by HL156A may be associated with inhibition of cell proliferation through decreasing the mitochondrial membrane potential or IGF-1/AKT/mTOR signaling or inducing AMPK signaling in FaDu and YD-10B cells.

Collectively, the results of the present study suggest that HL156A may have the potential to arrest the progression of oral cancer through suppression of the IGF/AKT/mTOR pathway or MMP-2 and MMP-9 pathways. In addition, AMPK activity, at least in part, is also required for the above-mentioned tumor suppression. In conclusion, the results clarify the beneficial effect of HL156A in reducing oral cancer development.

Collection @ chosun

조선대학교 CHOSUN UNIVERSITY

V. REFERENCES

1. Chin D, Boyle GM, Porceddu S, Theile DR, Parsons PG, Coman WB. Head and neck cancer: past, present and future. Expert Rev Anticancer Ther. 2006;6:1111-1118.

2. Mao L, Hong WK, Papadimitrakopoulou VA. Focus on head and neck cancer. Cancer Cell. 2004;5:311-316.

3. Hopper C, Kübler A, Lewis H, Tan IB, Putnam G. mTHPC-mediated photodynamic therapy for early oral squamous cell carcinoma. Int J Cancer. 2004;111:138-146.

4. Del Barco S, Vazquez-Martin A, Cufí S, et al. Metformin: multifaceted protection against cancer. Oncotarget. 2011;2:896-917.

5. Akinyeke T, Matsumura S, Wang X, et al. Metformin targets c-MYC oncogene to prevent prostate cancer. Carcinogenesis. 2013;4:2823-2832.

6. Amin S, Mhango G, Lin J, et al. Metformin improves survival in patients with pancreatic ductal adenocarcinoma and pre-existing diabetes: a propensity score analysis. Am J Gastroenterol. 2016;111:1350- 1357.

7. Thompson AM. Molecular pathways: preclinical models and clinical trials with metformin in breast cancer. Clin Cancer Res. 2014;20:2508-2515.

8. Hadad SM, Hardie DG, Appleyard V, Thompson AM. Effects of metformin on breast cancer cell proliferation, the AMPK pathway and the cell cycle. Clin Transl Oncol. 2014;16:746-752.

9. Colquhoun AJ, Venier NA, Vandersluis AD, et al. Metformin enhances the antiproliferative and apoptotic effect of bicalutamide in prostate cancer. Prostate Cancer Prostatic Dis. 2012;15:346-352.

10. Guo Y, Yu T, Yang J, et al. Metformin inhibits salivary adenocarcinoma

Collection @ chosun

조선대학교 CHOSUN UNIVERSITY

growth through cell cycle arrest and apoptosis. Am J Cancer Res. 2015;5:3600-3611.

11. Daugan M, Dufaÿ Wojcicki A, d'Hayer B, Boudy V. Metformin: An anti-diabetic drug to fight cancer. Pharmacol Res. 2016;113:675-685.

12. Sosnicki S, Kapral M, Wezglarz L. Molecular targets of metformin antitumor action. Pharmacol Rep. 2016;68:918-925.

13. Hadad SM, Fleming S, Thompson AM. Targeting AMPK: a new therapeutic opportunity in breast cancer. Crit Rev Oncol Hematol.2008;67:1-7.

14. Lee HS, Shin HS, Choi J, et al. AMP-activated protein kinase activator, HL156A reduces thioacetamide-induced liver fibrosis in mice and inhibits the activation of cultured hepatic stellate cells and macrophages. Int J Oncol. 2016;49:1407-1414.

15. Ju KD, Kim HJ, Tsogbadrakh B, et al. HL156A, a novel AMP-activated protein kinase activator, is protective against peritoneal fibrosis in an in vivo and in vitro model of peritoneal fibrosis. Am J Physiol Renal Physiol. 2016;310:F342-F350.

16. Choi J, Lee JH, Koh I, et al. Inhibiting stemness and invasive properties of glioblastoma tumorsphere by combined treatment with temozolomide and a newly designed biguanide (HL156A). Oncotarget. 2016;7:65643-65659.

17. Gottlieb E, Armour SM, Harris MH, Thompson CB. Mitochondrial membrane potential regulates matrix configuration and cytochrome c release during apoptosis. Cell Death Differ. 2003;10:709-717.

18. Wang CH, Wu SB, Wu YT, Wei YH. Oxidative stress response elicited by

Collection @ chosun

조선대학교 CHOSUN UNIVERSITY

mitochondrial dysfunction. Implication in the pathophysiology of aging. Exp Biol Med. 2013;238:450-460.

19. Moiseeva O, Deschênes-Simard X, St-Germain E, et al. Metformin inhibits the senescence-associated secretory phenotype by interfering with IKK/NF-jB activation. Aging Cell. 2013;12:489-498.

20. Nabeshima K, Inoue T, Shimao Y, Sameshima T. Matrix metalloproteinases in tumor invasion: role for cell migration. Pathol Int. 2002;52:255-264.

21. Gialeli C, Theocharis AD, Karamanos NK. Roles of matrix metalloproteinases in cancer progression and their pharmacological targeting. FEBS J. 2011;278:16-27.

22. Provinciali N, Lazzeroni M, Cazzaniga M, Gorlero F, Dunn BK, DeCensi A. Metformin: risk-benefit profile with a focus on cancer. Expert Opin Drug Saf. 2015;14:1573-1585.

23. Wu L, Zhu J, Prokop LJ, Murad MH. Pharmacologic therapy of diabetes and overall cancer risk and mortality: a meta-analysis of 265 studies. Sci Rep. 2015;5:10147-10157.

24. Bao B, Azmi AS, Ali S, Zaiem F, Sarkar FH. Metformin may function as anti-cancer agent via targeting cancer stem cells: the potential biological significance of tumor-associated miRNAs in breast and pancreatic cancers. Ann Transl Med. 2014;2:59-75.

25. Menendez JA, Quirantes-Pine R, Rodriguez-Gallego E, et al. Oncobiguanides: Paracelsus' law and nonconventional routes for administering diabetobiguanides for cancer treatment. Oncotarget. 2014;5:2344-2348.

Collection @ chosun

조선대학교 CHOSUN UNIVERSITY

26. Ashinuma H, Takiguchi Y, Kitazono S. Antiproliferative action of metformin in human lung cancer cell lines. Oncol Rep. 2012;28:8-14.

27. Cantrell LA, Zhou CX, Mendivil A, Malloy KM, Gehrig PA, Bae-Jump VL. Metformin is a potent inhibitor of endometrial cancer cell proliferation-implications for a novel treatment strategy. Gynecol Oncol. 2010;116:92-98.

28. Sikka A, Kaur M, Agarwal C, Deep G, Agarwal R. Metformin suppresses growth of human head and neck squamous cell carcinoma via global inhibition of protein translation. Cell Cycle. 2012;11:1374-1382.

29. Sesen J, Dahan P, Scotland SJ, et al. Metformin inhibits growth of human glioblastoma cells and enhances therapeutic response. PLoS ONE. 2015;10:e0123721.

30. Haugrud AB, Zhuang Y, Coppock JD, Miskimins WK. Dichloroacetate enhance apoptotic cell death via oxidative damage and attenuates lactate production in metformin-treated breast cancer cells. Breast Cancer Res Treat. 2014;147:539-550.

31. Johansson N, Ahonen M, Kähäri VM. Matrix metalloproteinases in tumor invasion. Cell Mol Life Sci. 2000;57:5-15.

32. Cui QL, Almazan G. IGF-I-induced oligodendrocyte progenitor proliferation requires PI3K/Akt, MEK/ERK, and Src-like tyrosine kinases. J Neurochem. 2007;100:1480-1493.

33. Guerrero-Zotano A, Mayer IA, Arteaga CL. PI3K/AKT/mTOR: role in breast cancer progression, drug resistance, and treatment. Cancer Metastasis Rev. 2016;35:515-524.

Collection @ chosun

조선대학교 CHOSUN UNIVERSITY

34. Yu JS, Cui W. Proliferation, survival and metabolism: the role of PI3K/AKT/mTOR signalling in pluripotency and cell fate determination. Development. 2016;143:3050-3060.

35. Jiao Q, Zou L, Liu P, et al. Xanthoceraside induces apoptosis in melanoma cells through the activation of caspases and the suppression of the IGF-1R/Raf/MEK/ERK signaling pathway. J Med Food. 2014;17:1070-1078.

36. Green CJ, Pedersen M, Pedersen BK, Scheele C. Elevated NF-jB activation is conserved in human myocytes cultured from obese type 2 diabetic patients and attenuated by AMP-activated protein kinase. Diabetes. 2011;60:2810-2819.

Collection @ chosun

조선대학교 CHOSUN UNIVERSITY

Ⅵ. 국문 초록

새로운 Metformin 유도체 HL156A가 IGF/AKT/mTOR 경로 저해를 통해 구강암 유도에 미치는 영향 연구

Lam Thuy Giang

지도교수: 안상건

조선대학교 대학원

치의생명공학과

제 2 형 당뇨병 환자를 위한 항 당뇨병 약물로 널리 알려진 biguanide 계열의 Metformin은 최근에 암 억제 능력이 있음을 보여주고 있다. 본 연구의 목적은 사람의 구강암 세포에 대한 새로운 Metformin 유도체인 HL156A의 효과를 조사하고 조절 메커니즘을 조사하는 것이다. 본 연구에서 HL156A는 FaDu 및 YD-10B의 Cell viability 및 colony agar formation을 농도 의존적으로 유의하게 감소시킴을 관찰하였다. HL156A는 구강암 세포의 migration과 invasion을 현저하게 감소시킬 뿐 아니라 HL156A가 reactive oxygen speies (ROS)을 유도하고 mitochondria membrane potential을 억제하였다. 또한 HL156A는 caspase-3 및 caspase-9 활성화를 통해 구강암 세포에서 세포사멸을 유도하였다. HL156A는 Insulin growth factor -1 신호 전달 기전에 관여하는 AKT, mTOR 및 ERK1/2 의 발현 및 활성화를 억제한 반면 AMP-activated protein kinase/ nuclear factor kappa B (AMPK/NF-κB) signaling을 유도하였다. 부가적으로, 이종 종양 이식 모델의 HL156A 처리 종양조직에서 HL156A가 p-IGF-1, p-mTOR 및 세포 증식인자인 proliferating cell nuclear antigen (PCNA)를 억제하고, p-AMPK의 발현이 유도됨으로서 AT84 마우스 구강 종양의 성장을 저해함을 보여주고 있다. 이러한 결과는 구강암의 치료 방법의 후보자로서의 새로운 Metformin 유도체 HL156A의 잠재적 가치를 시사한다.

Collection @ chosun